Transportmetrica B: Transport Dynamics

ISSN: 2168-0566 (Print) 2168-0582 (Online) Journal homepage: http://www.tandfonline.com/loi/ttrb20

Traffic flow sensitivity to parameters in viscoelastic modelling

M. N. Smirnova, A. Bogdanova, Zuojin Zhu & N. N. Smirnov

To cite this article: M. N. Smirnova, A. Bogdanova, Zuojin Zhu & N. N. Smirnov (2017) Traffic flow sensitivity to parameters in viscoelastic modelling, Transportmetrica B: Transport Dynamics, 5:1, 115-131, DOI: 10.1080/21680566.2016.1142402

To link to this article: http://dx.doi.org/10.1080/21680566.2016.1142402

Published online: 11 Apr 2016.

TRANSPORTMETRICA B: TRANSPORT DYNAMICS, 2017
VOL. 5, NO. 1, 115–131
http://dx.doi.org/10.1080/21680566.2016.1142402

Taylor & Francis
Taylor & Francis Group

Traffic flow sensitivity to parameters in viscoelastic modelling

M. N. Smirnova[a,b], A. Bogdanova[a], Zuojin Zhu[a,c] and N. N. Smirnov[a,d]

[a]Faculty of Mechanics and Mathematics, Moscow M.V. Lomonosov State University, Moscow, Russia; [b]Saint Petersburg State Polytechnical University, St. Petersburg, Russia; [c]Faculty of Engineering Science, University of Science and Technology of China, Hefei, People's Republic of China; [d]Scientific Research Institute for System Analysis, Russian Academy of Sciences, Moscow, Russia

ABSTRACT

This paper presents viscoelastic modelling of traffic flows briefly first and then shows numerical simulation results of ring traffic flow sensitivity to model parameters, such as viscoelasticity, average vehicle length, braking distance, and characteristic length used to define relaxation time. It was found that traffic flow pattern formation is dramatically sensitive to viscoelasticity and fundamental diagram which is explicitly impacted by average vehicle length and braking distance, implying that drivers' self-organisation ability is significant in determining the intensity of traffic wave interaction. Since the decrease of characteristic length can lead to a relevant change of traffic relaxation time, the length can play a sensitive role in changing traffic wave structures. Optimisation of traffic regulations is necessary for the well operation of a segmental or ring road.

ARTICLE HISTORY
Received 11 July 2015
Accepted 11 January 2016

KEYWORDS
Viscoelasticity; average vehicular length; braking distance; traffic flow sensitivity

1. Introduction

Traffic flow is a long time hot spot of academics in mathematical, physical, and civil-engineering societies, leading to the occurrence of many models. The probably simplest model LWR (Lighthill and Whitham 1955; Richards 1956) can capture primary features of traffic flows on highways (Kuhne and Michalopoulos 2001), be used in analysing interrupted traffic flow (Michalopoulos et al. 1984), develop macroscopic models and compare with real data in Paris (Papageorgiou and Blosseville 1989), and to construct the entropy solutions with a discontinuous fundamental diagram (Lu et al. 2009). The LWR extensions can certainly predict traffic hysteresis (Wong and Wong 2002), simulate evolution of density waves (Zhu and Wu 2003), and critical transition in bottleneck-related traffic (Chang and Zhu 2006), although the application results are not usually favourable.

Fundamentals of traffic operations have been described by Daganzo (1997). As soon as momentum conservation of vehicles is further considered in mathematical modelling, the proposed models are usually called high-order traffic flow models, among which that should be mentioned are the model of Payne (1971), the gas-kinetic-based model (Helbing and Treiber 1998; Hoogendoorn and Bovy 2000), the cluster effect model (Kerner and Konhäuser 1993; Hilliges and Weidlich 1995), and the generic model (Lebacque, Mammar, and Haj-Salem 2007b; Zhang, Wong, and Dai 2009; Lebacque and Khoshyaran 2013). High-order models are more favourable in simulating propagation performance of stop and moving waves in traffic flows. In contrast to the negative comment (Daganzo 1995), there are still many remarkable applications (Liu and Lyrintzis 1996; Zhang and Wong 2006; Ou and Dai 2006) and further developments (Klar and Wegener 2000; Aw and Rascle 2000; Zhang 2003; Kiselev et al. 2000, 2004; Zhang and Wong 2006; Lebacque, Mammar, and Haj-Salem 2007a; Li 2008; Mammar,

CONTACT Zuojin Zhu zuojin@ustc.edu.cn

Lebacque, and Salem 2009; Zhang, Wong, and Dai 2009; Ngoduy 2013; Zhu and Yang 2013; Tordeux et al. 2014; Costeseque and Lebacque 2014; Delis, Nikolos, and Papageorgiou 2014; Spiliopoulou et al. 2014; Smirnova et al. 2014a; Smirnov et al. 2014; Bogdanova et al. 2015; Hoogendoorn et al. 2016).

In traffic flow modelling, it should be mentioned that a phase diagram was explained by Helbing, Hennecke, and Treiber (1999), the diagram was obtained for the nonlocal, gas-kinetic traffic model in the study of a freeway having ramp effect and single perturbation. Some questions of traffic flows were answered by Helbing (2001) by using methods in statistical physics and non-linear dynamics of self-driven particle systems. By using average vehicle length and braking distance at free flow speed, an expression of traffic sound speed was derived (Kiselev et al. 2000). It was reported that for a VAZ-type vehicle, the analytically obtained sound speed agrees well with that experimentally measured in Lincoln Tunnel in New York.

To seek the travelling wave solution of a wide cluster, by using weak solution theory and the Payne–Whitham (PW) model (Payne 1971; Whitham 1974), it was found that the conservation form for the acceleration equation is an important ingredient in developing higher order traffic flow models (Zhang and Wong 2006). To describe traffic flow dynamics, by including the introduction of a pseudo-density transformed from the velocity, the pressure as a function of the pseudo-density, and the relaxation of velocity to equilibrium, three flow regimes have been considered by Zhang, Wong, and Dai (2009), for which, based on fundamental diagram reported by Castillo and Benitez (1995a,b), numerical examples were used to show the model ability in reproducing some notable traffic phenomena. For travelling wave solutions described by the PW model, a stability analysis (Li 2008) has revealed that the solutions are asymptotically stable under small disturbances and under sub-characteristic condition.

Using the gas-kinetic-based approach (Helbing and Treiber 1998; Hoogendoorn and Bovy 2000; Ngoduy 2012), a macroscopic model has been developed (Ngoduy 2013), in the traffic flow intelligent vehicles are moving closer to each other than manual vehicles and operating in a form of many platoons each of which contains several vehicles. Tordeux et al. (2014) have reported the main aspects of a stochastic conservative model of the evolution of the number of vehicles per road section. The model defined in continuous time on a discrete space follows a misanthrope Markovian process.

Combining the LWR model with dynamics of driver-specific attributions, generic second-order modelling (GSOM) family of traffic flow models can be expressed as a system of conservation laws, as reported by Lebacque and Khoshyaran (2013). They have indicated that a proper Lagrangian formulation of the GSOM model can be recast as a Hamilton–Jacobi equation, the solution of which can be expressed as the value function of an optimal control problem. For models of the GSOM family, Costeseque and Lebacque (2014) have proved a variational principle, obtained an adequate framework for effective numerical methods, and shown the method efficiency through a numerical test. For essentially unsteady-state traffic flows wherein massive changing of lanes produces an effect on handling segmentary road capacity, a mathematical model has been developed recently (Smirnova et al. 2014a; Smirnov et al. 2014). The model has no analogue with classical hydrodynamics, because momentum equations in the flow direction and in orthogonal directions of lane-changing are explicitly different.

In this paper, the viscoelastic traffic flow model (Smirnova et al. 2014b; Bogdanova et al. 2015) is used to explore traffic flow sensitivity to parameters, such as viscoelasticity, average vehicle length, braking distance, and characteristics length of flows used to define traffic relaxation time. The traffic model is briefly introduced at first, where viscosity and elasticity, sound speed and relaxation time of traffic flows are used in modelling. Then on the basis of the traffic model, with the total variation diminishing (TVD) scheme (Roe 1981), numerical tests for ring traffic flows are carried out to obtain traffic flow patterns, speed and density evolutions and instantaneous speed–density relations at a given observation station. By changing values of viscoelasticity, average vehicle length, braking distance, and characteristic length of flows, the test results for ring traffic flows are shown to reflect the traffic flow sensitivity. To the best knowledge of authors, despite the special concern of the fundamental diagram (Haight 1963; Daganzo 1997; Lebacque, Mammar, and Haj-Salem 2007b; Zhang, Wong, and

Dai 2009; Lebacque and Khoshyaran 2013), sofar traffic flow sensitivity to these parameters has been less reported.

2. Viscoelastic model

Here, we briefly repeat some model descriptions given by Bogdanova et al. (2015). Traffic flow has a self-organising behaviour, as drivers can usually adjust the moving speed so that the time headway can approach $1/q_e$ when the instantaneous traffic flow rate (q) is unequal to the equilibrium one (q_e) (Castillo 2001). This self-organising behaviour has been considered in cluster effect models (Kerner and Konhäuser 1993; Hilliges and Weidlich 1995). Vehicular interaction is relatively intense in congested traffic flows, it can generate a synchronised flow mode wherein flow rate is oscillating or a jam occurs (Kerner and Konhäuser 1993). However, the flow is further homogeneous and stable for denser flow situation when the traffic speed is less than the second critical speed at density ρ_{c2} (Schönhof and Helbing 2009) (Figure 1).

As relaxation time is a long time used in expressing external force of traffic flows, while relaxation and elastic process are related intrinsically from the points of views of fluid mechanics, it is therefore more reasonable to further include the elastic effect in traffic flow modelling. In the present viscoelastic traffic flow modelling, only the interaction between the lead and follower vehicles is involved, the lane interaction is neglected. Hence, traffic flow rate and density are one-dimensional variables.

To simplify description, different from the previous work (Smirnova et al. 2014b; Bogdanova et al. 2015), the model given below has assumed that ramp effect can be excluded, while other assumptions remain the same, i.e. (i) road capacity is driver-independent and (ii) traffic flows satisfy a linear viscoelastic constitutive relationship. The second assumption is made mainly because relaxation time has been used in many high-order modelling, itself is a concept reflecting elastic and viscous properties of fluids (Han 2000), and drivers' concern of driving safety induces the motion of vehicles has a memory behaviour. Therefore, it is comparatively appropriate to describe this traffic performance with a memory function.

In non-Newtonian fluid mechanics, the shear stress of linear viscoelastic fluid flow is:

$$\mathbf{T}_s = \int_0^{\infty} f(s)\mathbf{H}(s)\,\mathrm{d}s \tag{1}$$

here $f(s)$ is the memory function. Based on the experimental observation of the relaxation of shear stress of macromolecule polymer and the theory of micro-rheology (Wagner 1978), we can write the memory function $f(s)$ in the following form:

$$f(s) = G\sum_{1}^{N}\frac{1}{\tau_j}\exp\left(-s/\tau_j\right) \tag{2}$$

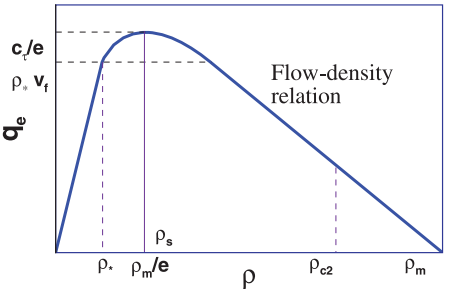

Figure 1. Fundamental diagram used in Kiselev et al. (2000).

Here G is the modulus of fluid elasticity, and τ_j is the relaxation time with the jth order. Hence, the traffic flow modelling can be started from the linear viscoelastic constitutive equation:

$$\mathbf{T} = -p\mathbf{I} + G\sum_{j=1}^{N}\int_0^{\infty}\frac{1}{\tau_j}\exp(-s/\tau_j)\mathbf{H}(s)\,\mathrm{d}s \tag{3}$$

where $\mathbf{T}(= -p\mathbf{I} + \mathbf{T}_s)$ and p are, respectively, the stress tensor and traffic pressure. $\mathbf{H}(s)$ is the Finger deformation tensor. For the maximum relaxation order denoted by N, the Finger deformation tensor is given by $\mathbf{H}(s) = \sum_{k=1}^{N}(-1)^{k+1}(s^k/k!)\mathbf{B}_k$, where $\mathbf{B}_k$ is the White–Metzner tensor and s is the elapsed time period (Han 2000).

In the analogy to model unsteady traffic flows, using the first-order approximation in the case of $N = 1$, and the integration formula $\int_0^{\infty} s^k \exp(-as)\,\mathrm{d}s = k!/a^{k+1}$ merely valid for the positive integer k and the positive real number a, the traffic flow stress is:

$$T = -p + G\tau B_1 \tag{4}$$

Denoting traffic flow velocity by u, then, according to Appendix 1, we have $B_1 = 2u_x$ and then $\rho\nu = 2G\tau$, $T = -p + \rho\nu u_x$. For the case of $N = 2$, the relevant traffic flow model has been reported (Zhu and Yang 2013). With respect to existing high-order models, the general form of the forces acting on vehicular clusters can be written as:

$$F = (q_e - q)/\tau + T_x \tag{5}$$

where the subscribe 'e' represents the relevant variables under equilibrium traffic state, q_e is the equilibrium traffic flow rate which can be seen as a function of traffic density, with the form relating to free flow speed v_f, the first critical density ρ_*, vehicular jam density ρ_m, and vehicular moving speed parameter c_τ as reported (Kiselev et al. 2000). Some examples used to describe speed–flow–density relationships for freeway analysis can be found in McShane, Roess, and Prassas (1998). T_x is the relevant surface force related to the traffic stress.

For simplicity, we use the traffic fundamental diagram used in Kiselev et al. (2000), it can be written as:

$$q_e = \begin{cases} v_f\rho & \text{for } \rho \le \rho_* \\ -c_\tau\rho\ln(\rho/\rho_m) & \text{for } \rho_* < \rho \le \rho_m \end{cases} \tag{6}$$

As seen in Appendix 2 and Smirnova et al. (2014b), the traffic pressure has the form:

$$p = p_m(1-\alpha)(\rho/\rho_m)/[1-\alpha(\rho/\rho_m)] \tag{7}$$

The maximum permissible density at free flow speed v_f is given by:

$$\rho_* = \rho_m\exp(-v_f/c_\tau) \tag{8}$$

which can be directly derived from the traffic state equation (6) by letting ρ approach $\rho*$. Because the safe traffic density itself indicates that the distance between vehicles is *longer* than braking distance $X(v_f)$, the density ρ_* should be defined by the equality:

$$\rho_* = \rho_m[1 + X(v_f)/l]^{-1} \tag{9}$$

Over which traffic flow becomes unstable, therefore it can also be called the first critical density, or the first transitional density. Hence, combining Equations (8) and (9) gives the length ratio $[X(v_f)/l]$-dependent speed:

$$c_\tau = v_f/\ln[1 + X(v_f)/l] \tag{10}$$

The traffic state equation (6) is shown in Figure 1, where $e \approx 2.71828$, ρ_{c2} is the second critical traffic density, over which the traffic flow becomes stable again.

Note that in the traffic pressure definition (7), $\alpha = l\rho_m$, l is average vehicle length, ρ_m, p_m are jam density and jam pressure, with v_f denoting the free flow speed. Note that the flow–density relation used for illustrating traffic fundamental diagram, usually called traffic state equation, explicitly has a crucial impact on the traffic road operation (Haight 1963). For the urban traffic, based on analysis of the third-order spline curve used to denote fundamental diagram, a single parameter state equation has been reported and discussed (Zhu et al. 2002).

It is necessary to remind that traffic pressure is just a notation, it does not exist physically (Smirnova et al. 2014a; Smirnov et al. 2014). Therefore, virtual attraction and repulsion forces are introduced, which for one-dimensional flow could be represented as a derivative of some function, by fluid flow analogy, it is named traffic pressure. This viewpoint has been appropriately used in mathematical modelling of traffic flows (Smirnova et al. 2014b).

By assuming the traffic pressure is proportional to the reciprocal of spatial headway of vehicles rather than the traffic density directly, and assuming the traffic jam pressure is approximately identical to the total traffic pressure at the transitional point ρ_*, as shown in Appendix 2, we have traffic jam pressure:

$$p_m = \frac{(1 - \alpha\rho_*/\rho_m)\rho_*/\rho_m}{2(1 - \rho_*/\rho_m)} v_f^2 \cdot \rho_m = c_0^2 \rho_m \tag{11}$$

with:

$$c_0^2 = \frac{(1 - \alpha\rho_*/\rho_m)\rho_*/\rho_m}{2(1 - \rho_*/\rho_m)} v_f^2 \tag{12}$$

As shown in Appendix 2, using sound speed definition in fluid dynamics, we can derive a traffic sound speed:

$$c = c_0\sqrt{1 - \alpha}/(1 - \alpha\rho/\rho_m) \tag{13}$$

For the pressure-spatial headway dependency, merely there is a reasonability theoretically. Justifications in reality require further explorations. As soon as spatial headway tends to zero, the traffic pressure approaches infinity, implying the local vehicles should be stopped abruptly. The assumption of jam pressure is made just for the sound speed derivation.

Therefore, the viscoelastic traffic flow modelling gives rise to the governing equation:

$$\begin{aligned} \rho_t + q_x &= 0 \\ \rho(u_t + uu_x) &= R \end{aligned} \tag{14}$$

where R satisfies the following equation:

$$R = \rho(u_e - u)/\tau - c^2\rho_x + [(2G\tau)u_x]_x \tag{15}$$

Assume that the product of relaxation time and sound speed is unchangeable, we yield a density-dependent relaxation time:

$$\tau = \tau_0(1 - \alpha\rho/\rho_m)/\sqrt{1 - \alpha} \tag{16}$$

where $\tau_0 = l_0/c_\tau$, l_0 denotes a characteristic length scale of traffic flows. Explicitly, the relaxation time decreases linearly with traffic density, which should be consistent with the general view of travellers.

The primary difference of the present traffic model from the viscoelastic model reported elsewhere (Zhu and Yang 2013) is that the model uses the first-order analogy approximation, the non-triangular traffic flow–density relationship, such as used by Kiselev et al. (2000), and includes the traffic ramp effect. In the present model, the traffic pressure, viscosity, relaxation time, and sound speed have been described individually.

3. Linear stability analysis

The linear stability analysis is presented by using the linear stability theory of Chandrasekhar (1961). Hence, we express the variables with their exponential type disturbances as:

$$\rho = \rho_0 + \tilde{\rho}\exp(\omega t + ikx) \tag{17a}$$

$$u = u_0 + \tilde{u}\exp(\omega t + ikx) \tag{17b}$$

$$q = q_0 + \tilde{q}\exp(\omega t + ikx) \tag{17c}$$

where the subscript '0' refers to the base state of traffic flow, with the magnitude of the flow rate disturbance given by the supplementary expression $\tilde{q} = u_0\tilde{\rho} + \rho_0\tilde{u}$, and:

$$q_e(\rho) = q_e(\rho_0) + q_e'(\rho_0)\tilde{\rho}\exp(\omega t + ikx) \tag{18}$$

where $q_e(\rho_0) = \rho_0 u_0$. We can derive the dispersion relation as:

$$\omega^2 + (C + i2ku_0)\omega + ik[Cu_0 + C_{1R} + i(C_{1I} + ku_0^2)] = 0 \tag{19}$$

where $q_e' = dq_e/d\rho$, and:

$$C = \left(\tau^{-1} + \frac{2G\tau}{\rho_0}k^2\right) \tag{20a}$$

$$C_1 = C_{1R} + iC_{1I} = (q_e' - u_0)\tau^{-1} - ikc^2 \tag{20b}$$

Substituting these variables in the viscoelastic traffic model, a criterion of traffic flows can be written as (Zhu and Yang 2013):

$$|J| = \left|\frac{q_e' - u_0}{c}\right| \le 1 + \left(\frac{2G\tau}{\rho_0}\right)k^2 \tag{21}$$

When the inequality (21) is satisfied, the traffic flow is stable; and when we choose $2G\tau/\rho_0 = \nu, c = c_0$, the result is the same as what derived preciously (Payne 1979). It is clear that for $\rho \le \rho_*, q_e' = v_f = u_0$, vehicles are moving at free flow speed, the traffic flow is stable. Hence, as shown in Figure 1, ρ_* is called first critical density of traffic flows. Now it is clear that there is again the second critical density beyond which flows from unstable regime become stable regime under dense traffic flow situation (Schönhof and Helbing 2009; Zhang, Wong, and Dai 2009; Zhu and Yang 2013).

4. Numerical method

Letting the mandatory variables be ρ and q, and $R_1(= R + c^2\rho_x)$ instead of R, the governing Equation (14) becomes:

$$\frac{\partial \mathbf{U}}{\partial t} + \frac{\partial \mathbf{F}(U)}{\partial x} = \mathbf{S} \tag{22}$$

where $\mathbf{U} = (\rho, q)^{\mathrm{T}}$, $\mathbf{F(U)} = (q, q^2/\rho + p)^{\mathrm{T}}$, and $\mathbf{S} = (0, R_1)^{\mathrm{T}}$, with superscript 'T' representing vector transpose.

Equation (22) indicates that the two eigenvalues should be λ_k $(k = 1, 2)$, with $\lambda_1 = u - c$ and $\lambda_2 = u + c$, since the Jacobian matrix is given by:

$$\mathbf{A} = \begin{pmatrix} \frac{\partial F_1}{\partial U_1} & \frac{\partial F_1}{\partial U_2} \\ \frac{\partial F_2}{\partial U_1} & \frac{\partial F_2}{\partial U_2} \end{pmatrix} = \begin{pmatrix} 0 & 1 \\ -u^2 + c^2 & 2u \end{pmatrix} \tag{23}$$

Note that there is a controversy for the eigenvalues. Some claim that the eigenvalue should not exceed traffic speed, others do not employ this rule in traffic flow modelling. Actually, the present viscoelastic

model uses non-Newtonian fluid dynamics analogy but not the car-following constraint, the traffic speed is involving vehicular cluster rather than a single car. Hence, we tend to take the view that the eigenvalue limit is unnecessary.

The TVD scheme (Roe 1981) is used to seek numerical solutions of Equation (22), as the TVD scheme is easy to be implemented in coding. It should be mentioned that a family of spatial discretisations, including a second-order MUSCL scheme, and a fifth-order WENO scheme (Jiang and Shu 1996), and a detailed formulation of the scheme, has been presented in the research work of high-resolution numerical relaxation approximations to second-order macroscopic traffic flow models (Delis, Nikolos, and Papageorgiou 2014).

Denoting the space grid and the ratio of time step to grid step, respectively, by x_i and $\omega = \Delta t/\Delta x$, the numerical stability condition of TVD is:

$$\omega \cdot \max|\lambda_{k,i+1/2}| < 1, \quad k = 1, 2, \quad i = 0, 1, 2, \ldots, N-1 \tag{24}$$

where $\lambda_{k,i+1/2}$ represents the kth eigenvalue for $\mathbf{A}$ at $x_{i+1/2}$, N is the maximum of space grid number.

The term R_1 is calculated at the time level t^n with a linear expansion of:

$$R_1^{n+1/2} = R_1^n + \frac{1}{2}\left(\frac{\partial R_1}{\partial \rho}\right)\delta\rho^n + \frac{1}{2}\left(\frac{\partial R_1}{\partial q}\right)\delta q^n \tag{25}$$

where $\delta\rho^n = \rho^{n+1} - \rho^n$, $\delta q^n = q^{n+1} - q^n$. Representing the speed and length scales, respectively, by v_0 and $\Delta x(= l_0)$, we have:

$$\frac{\partial R_1}{\partial \rho} = \tau^{-1}\left(\frac{\partial q_e}{\partial \rho}\right), \quad \frac{\partial R_1}{\partial q} = -\tau^{-1} \tag{26}$$

The TVD scheme has the form:

$$\delta\mathbf{U}_i^n = -\omega(\hat{\mathbf{F}}_{i+1/2} - \hat{\mathbf{F}}_{i+1/2}) + (\Delta t)\mathbf{S}_i^n + \frac{\Delta t}{2}\left(\frac{\partial \mathbf{S}}{\partial \mathbf{U}}\right)_i^n \delta\mathbf{U}_i^n \tag{27}$$

where $\Delta t(= t^{n+1} - t^n)$. The numerical flux $\hat{\mathbf{F}}_{i+1/2}$ can be calculated by using the left and right eigen vectors of Jacobian matrix A. The calculation of $\hat{\mathbf{F}}_{i+1/2}$ involves the coefficient of the viscous term $Q_k(z)$ with a small artificial parameter ϵ_k. Some details for the case of vanished source $\mathbf{S}$ can be found in the previous work (Zhu and Wu 2003; Chang and Zhu 2006). In the calculation of $\Delta_k[= \omega(\hat{F}_{k,i+1/2} - \hat{F}_{k,i+1/2})$ for $k = 1, 2]$, $\rho_{i+1/2}$ and $q_{i+1/2}$ are calculated on the basis of Shui (1998), as reported by Bogdanova et al. (2015).

5. Results and discussion

5.1. Simulation parameters

To seek traffic flow sensitivity to parameters in the viscoelastic modelling, numerical simulations by virtue of the TVD (Roe 1981; Shui 1998) scheme were conducted for ring traffic without ramps' influences. Parameters of ring traffic operations are shown in Table 1. Periodic boundary condition is used, implying that solutions at $x_N(= 750)$ are superposed on those at x_0. The ring road with length $x_N = 750$ has a length unit $l_0 = 160$ m, excluding some cases wherein l_0 is permitted to be changeable for the sensitivity seeking work. The length l_0 determines the total ring road length for a given total grid

Table 1. Parameters of ring traffic operations.

v_f (km h^{-1})	ρ_m (veh km^{-1})	$X(v_f)$ (m)	l (m)	l_0 (m)	x_A	x_B	x_C	x_N
110	150	50	5.8	160	125	375	625	750

Table 2. Parameters used in numerical tests.

Case	l (m)	X (m)	l_0 (m)	ρ_*/ρ_m	t_0 (s)	τ_0 (s)	$\hat{G}_{\tau 0} = \left[\frac{2G(\tau_0 v_0)}{l_0^2} \cdot \frac{t_0}{q_0}\right]$[a]
1	6.3	50	160	0.1119	47.795	11.468	0.0625
2	5.8	50	160	0.1039	50.377	11.854	0.0625
3	5.3	50	160	0.0958	54.636	12.280	0.0625
4	4.8	50	160	0.0876	59.782	12.751	0.0625
5	5.8	55.8	160	0.0942	55.614	12.372	0.0125
6	5.8	50	160	0.1039	50.377	11.584	0.0125
7	5.8	44.2	160	0.1160	45.141	11.280	0.0125
8	5.8	38.4	160	0.1312	39.90	10.634	0.0125
9	5.8	50	160	0.1039	50.377	11.854	0.125
10	5.8	50	120	0.1039	37.783	8.891	0.125
11	5.8	50	100	0.1039	31.486	7.409	0.125
12	5.8	50	80	0.1039	25.189	5.927	0.125

[a] Respectively, the flow rate, speed, and time scales are $q_0 = \rho_* v_f$, $v_0 = l_0/t_0$, and $t_0 = l_0\rho_m/q_0$.

number N. The velocity scale is $v_0 = q_0/\rho_m (= v_f\rho_*/\rho_m \approx 3.176\,\text{m/s})$, corresponding to the time scale $t_0 = l_0/v_0$ (s), its value is given in Table 2. The initial density is given by:

$$\rho(0,x) = \begin{cases} 1 & \text{for } x \in [x_l - 1, x_l + 1] \\ 1/3 & \text{otherwise} \end{cases} \tag{28}$$

where the subscript l can be A, B and C, and initial flow rate $q(0,x) = q_e(\rho(0,x))$, can be calculated by Equation (6). As the section positions shown in Figure 2, x_l $(l = A, B, C)$ is assigned by values given in Table 1.

For average vehicle length $l = 5.8$ m, the traffic jam density is about 150 veh m^{-1}, corresponding to a minimal distance between jammed vehicles was assigned to be 0.86$\dot{6}$ m (Smirnova et al. in press). While for $v_f = 110$ km h^{-1}, based on the discussion with some experienced drivers in China, the braking distance of vehicles is assumed to be about 50 m, the distance has occurred in Equations (9) and (10) for describing ρ_* and c_τ, respectively. For a fixed characteristic length l_0, the relaxation time τ_0 is $\tau_0 (= l_0/c_\tau)$, the normalised viscoelasticity is $\hat{G}_{\tau 0} [= 2G(\tau_0 v_0)/l_0^2 \cdot t_0/q_0]$, as shown in Table 2. The ratio of time step to space grid step denoted by ω is set with a Courant number of 0.75 (Shui 1998), i.e. $\omega = 0.75/\max|\lambda_{k,i+1/2}|$, for $k = 1,2$, $i = 0, 1, 2, \ldots, N-1$.

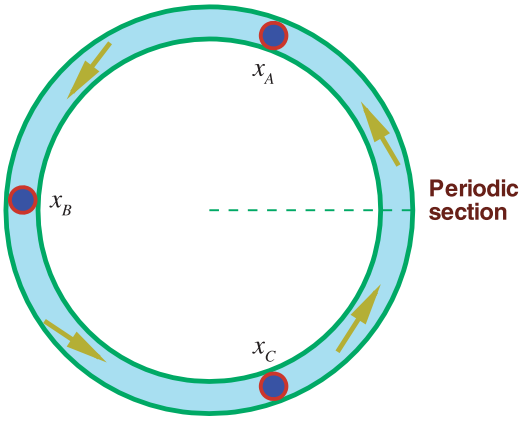

Figure 2. Schematic of the ring traffic flow without ramps.

5.2. Viscoelasticity effect

Changing the viscoelasticity $\hat{G}_{\tau 0}$ produces dramatically different flow patterns, as shown in Figure 3(a) and 3(b). In the case of smaller viscoelasticity $\hat{G}_{\tau 0} = 0.0125$, self-organising ability of drivers seems to be lower, the predicted flow pattern in Figure 3(a) has red coloured regions, suggesting that the speed in the red region is beyond $0.618 v_f$. Comparing the flow patterns in part (a) and part (b) of Figure 3, we can see that at any given time, the magnitude of spatial speed waves has a higher variation range; at any given section the temporal speed waves have a similar property of magnitude variation, implying there is a more intense interaction of traffic waves.

However, increasing viscoelasticity $\hat{G}_{\tau 0}$ to 0.125, as shown in Figure 3(b), in a large percent of the $t-x$ plane the flow pattern is observed to be approximately green coloured, suggesting that vehicles on ring road move usually at a speed $[0.5 \pm 0.05]$ in the unit of v_f, interaction of traffic wave has weakened due to the enhancement of drivers' self-organising ability. This indicates there is a demand of optimising traffic regulations for a given segmental road and condition of traffic operation.

5.3. Average vehicle length effect

As seen in Table 2, when average vehicle length decreases from 6.3 to 4.8 m with an interval of 0.5 m, the first critical density of traffic flows also decreases from 0.1119 to 0.0876 in the unit of ρ_m, indicating that the fundamental diagram curve has relevantly changed with average vehicle length. As shown in Figure 4(a)–(d), there are explicitly different forms of traffic flow pattern, driver-dependent fundamental diagram does have a determinant impact on spatial and temporal evolutions, from another research angle providing the numerical evidence for the reasonability of recent generic modelling (Lebacque, Mammar, and Haj-Salem 2007b; Zhang, Wong, and Dai 2009; Lebacque and Khoshyaran 2013). Mathematically, the choice of average vehicle length determines the form of source term R in momentum equation (14). Hence even though the initial and boundary conditions are the same, the numerically predicted spatial–temporal evolutions should be no doubt different.

Comparison of speed at $x = 375$ with existing measured data abstracted from McShane, Roess, and Prassas (1998) can be seen in Figure 5(a)–(d). The instantaneous speed was plotted as a function of density together with the equilibrium speed. As indicated by flow patterns in Figure 4(a)–(d), with the decrease of average vehicle length, on the ring road vehicles move at a smaller density variable range, or we can say traffic speed waves have smaller magnitudes. In particular, for $l = 6.3$ m, with a minimal distance of jammed vehicles $0.36\dot{6}$ m, as seen in Figure 5(a), the traffic state prevails in the larger area region, density can be as small as $0.13\rho_m$, at a given density the deviation between instantaneous speed u and equilibrium speed u_e is much larger than that in the case of $l = 4.8$ m.

5.4. Braking distance effect

Braking distance has also been employed in gas-kinetic-based modelling (Helbing and Treiber 1998). However, so far less discussion of its impact on flow pattern formation has been reported, although

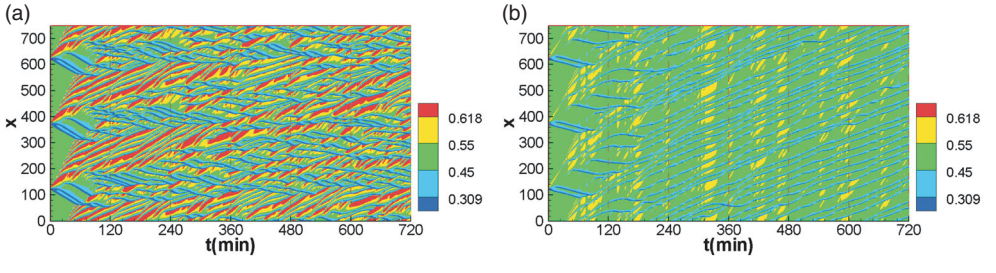

Figure 3. Traffic flow patterns illustrated by speed contours in the $t-x$ plane for $\hat{G}_{\tau 0} = 0.0125$ and $\hat{G}_{\tau 0} = 0.125$ (a and b), respectively.

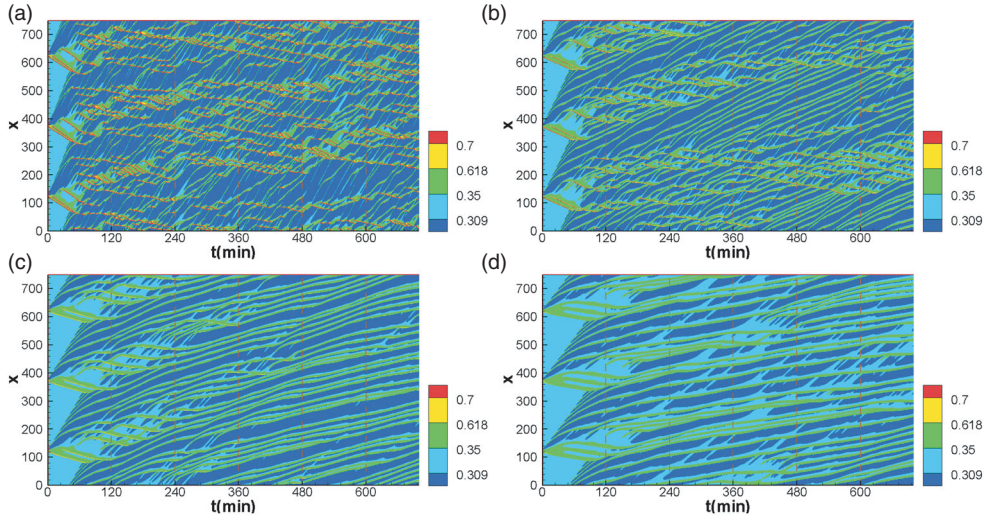

Figure 4. Traffic flow patterns illustrated by density contours in the $t-x$ plane for $l = 0.63$, 5.8, 5.3, and 4.8 m (a–d), respectively.

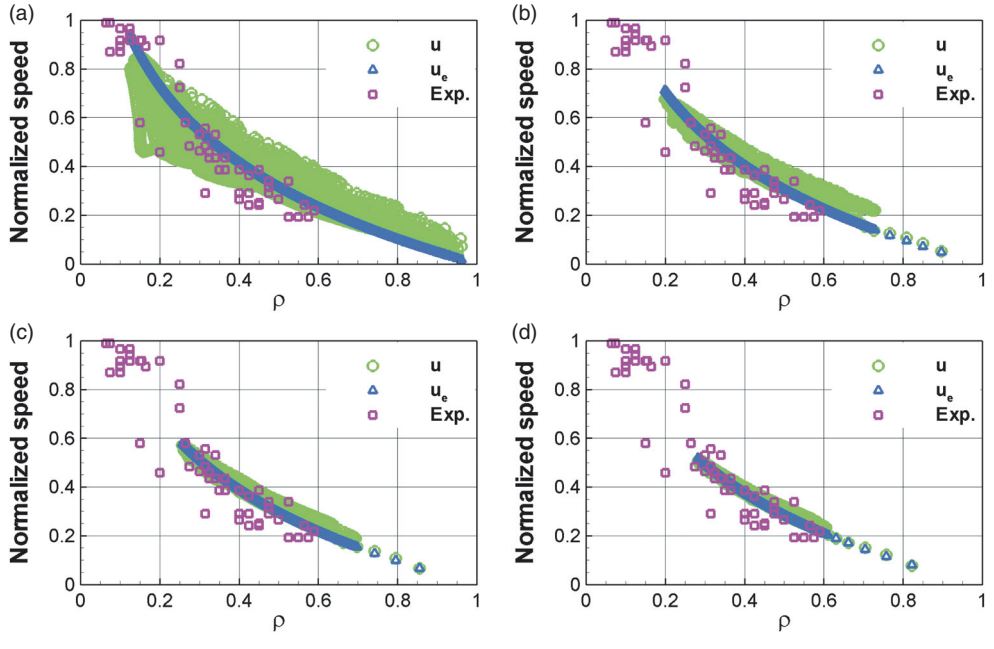

Figure 5. Comparison of traffic speed with existing measured data at $x = 375$ for $l = 0.63$, 5.8, 5.3, and 4.8 m (a–d), respectively. The observation data are abstracted from McShane, Roess, and Prassas (1998), and the jam density in density normalisation is supposed to be 200 veh mile^{-1}.

most of the drivers have recognised and understood that braking technology is a dominant feature of safety control. It is noted that in addition to using braking distance (Kiselev et al. 2000; Smirnova et al. 2014b; Bogdanova et al. 2015), emergency braking deceleration and maximal positive acceleration have been used in recent traffic flow modelling (Smirnova et al. 2014b; Smirnov et al. 2014; Smirnova et al. in press).

As seen in Figure 6(a)–(d), braking distance has a significant influence on traffic wave interaction on the ring road, because varying braking distance has generated significantly different flow patterns.

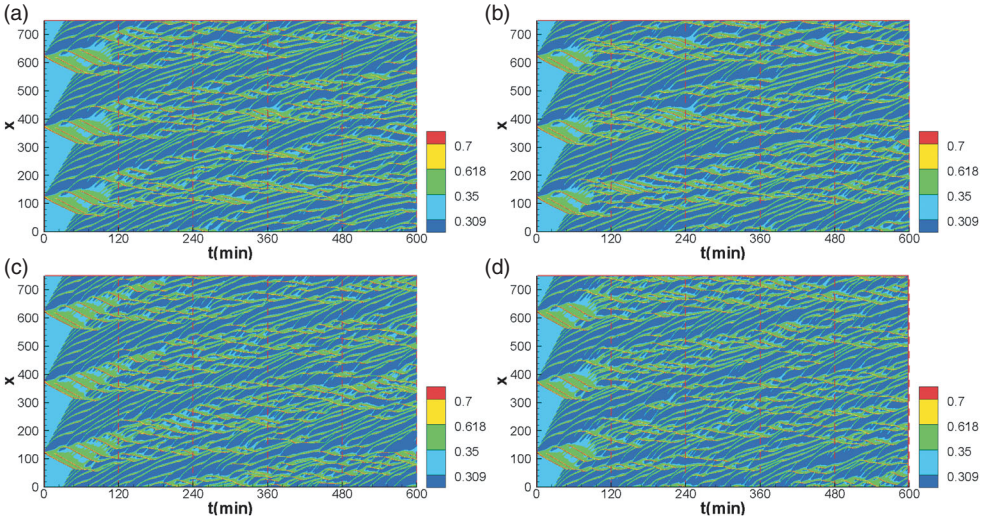

Figure 6. Traffic flow patterns illustrated by density contours in the $t-x$ plane for $X(v_f) = 55.8$, 50, 44.2, and 38.4 m (a–d), respectively.

As can be seen in Table 2, when the braking distance X decreases from 55.8 to 38.4 m with an interval of average vehicle length 5.8 m, the first critical density of traffic flows increases from 0.0942 to 0.1312 in the unit of jam density ρ_m, the relaxation time τ_0 also decreases from 12.372 to 10.634 s, implying that the equilibrium speed $u_e(= q_e/\rho)$ is sensitive, to the braking distance X as the flow q_e is described

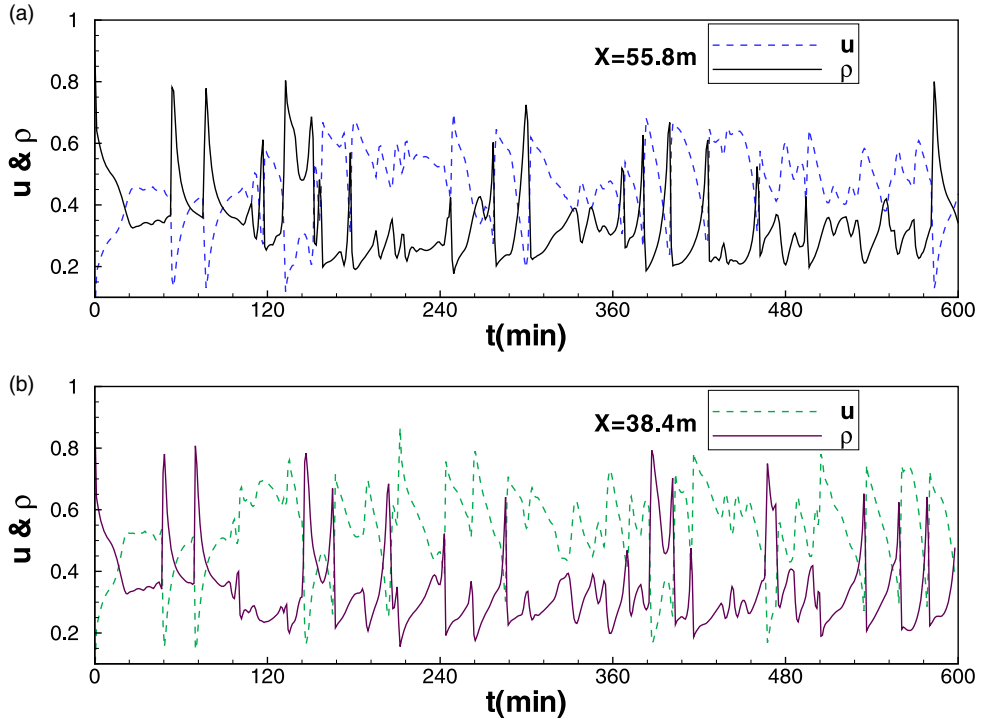

Figure 7. Evolutions of traffic speed and density at $x = 375$ for braking distance $X = 55.8$ m (a) and 38.4 m (b), respectively.

by length ratio-dependent speed c_τ given by Equation (10). The variation trends of ρ_* and τ_0 with the decrease of braking distance X are the reverse to that with the decrease of average vehicle length l. The sensitivity of braking distance X can be carefully observed from the predicted four traffic patterns shown in Figure 6, for which the normalised viscoelasticity $\hat{G}_{\tau 0}$ is fixed at 0.0125 as shown in Table 2.

To see the braking distance effect more clearly, temporal evolutions are shown in Figure 7(a) and 7(b). Obviously, the speed and density evolution curve at $x = 375$ in the case of $X = 38.4$ m are certainly different from that in the case of $X = 55.8$ m. For the given time range $t \in [0, 600]$ (min), the X induced differences occur not only in temporal wave shape, but also in the temporal wave period and magnitude.

Corresponding to the temporal evolutions given by Figure 7(a) and 7(b), instantaneous traffic speeds were plotted as a function of traffic density with the equilibrium speed in Figure 8, from which, the change of braking distance has caused a relevant change of fundamental diagram, which is reflected by the dependence of equilibrium speed u_e on traffic density ρ. For the case of $X = 55.8$ m, the dependence curve is shown by non-filled blue delta symbols; while for $X = 38.4$ m it is shown by non-filled green gradient symbols.

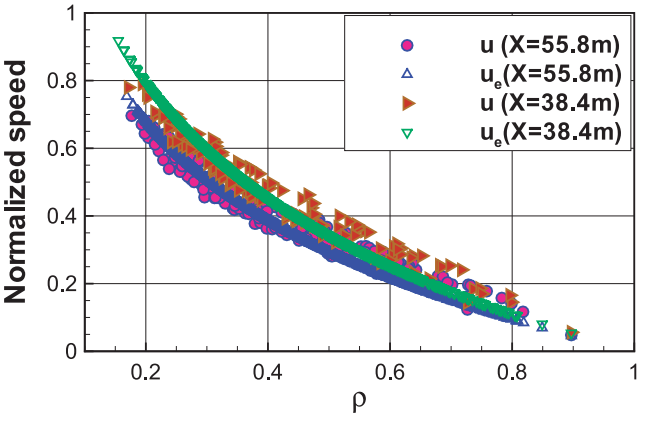

Figure 8. Comparison of traffic speed–density relation at $x = 375$ for braking distance $X = 55.8$ m and 38.4 m, respectively.

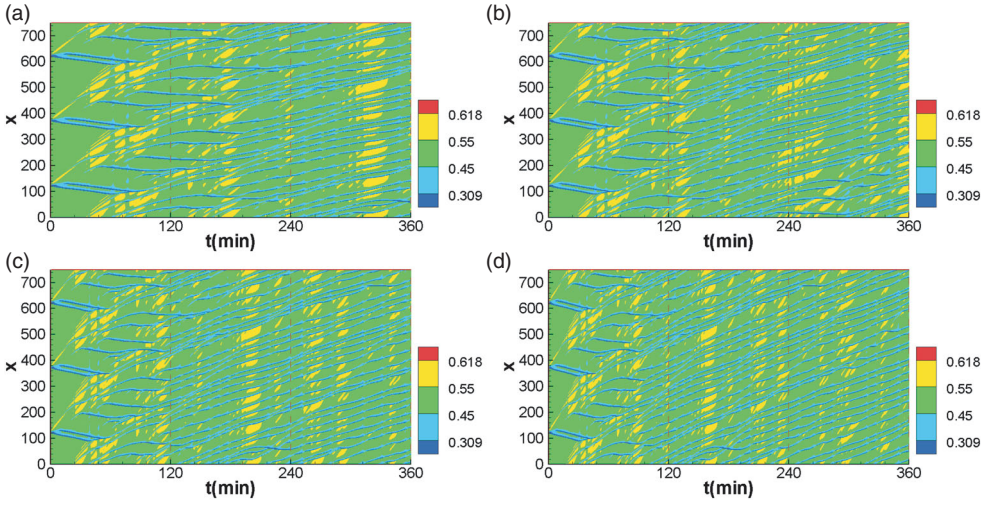

Figure 9. Traffic flow patterns illustrated by speed contours in the $t-x$ plane for $l_0 = 160$, 120, 100, and 80 m (a–d), respectively.

5.5. Characteristic length effect

Varying characteristic length l_0 leads to the occurrence of different flow patterns, which is shown by speed contours in Figure 9(a)–(d). Decreasing the length l_0 from 160 to 80 m, the related relaxation time decreases from 11.854 to 5.927 s. The traffic wave structure in the $t-x$ plane should be closely related to the l_0 assign, since the external force of traffic flow is described by the relaxation time term $[\rho(u_e - u)/\tau]$, as seen in Equation (15).

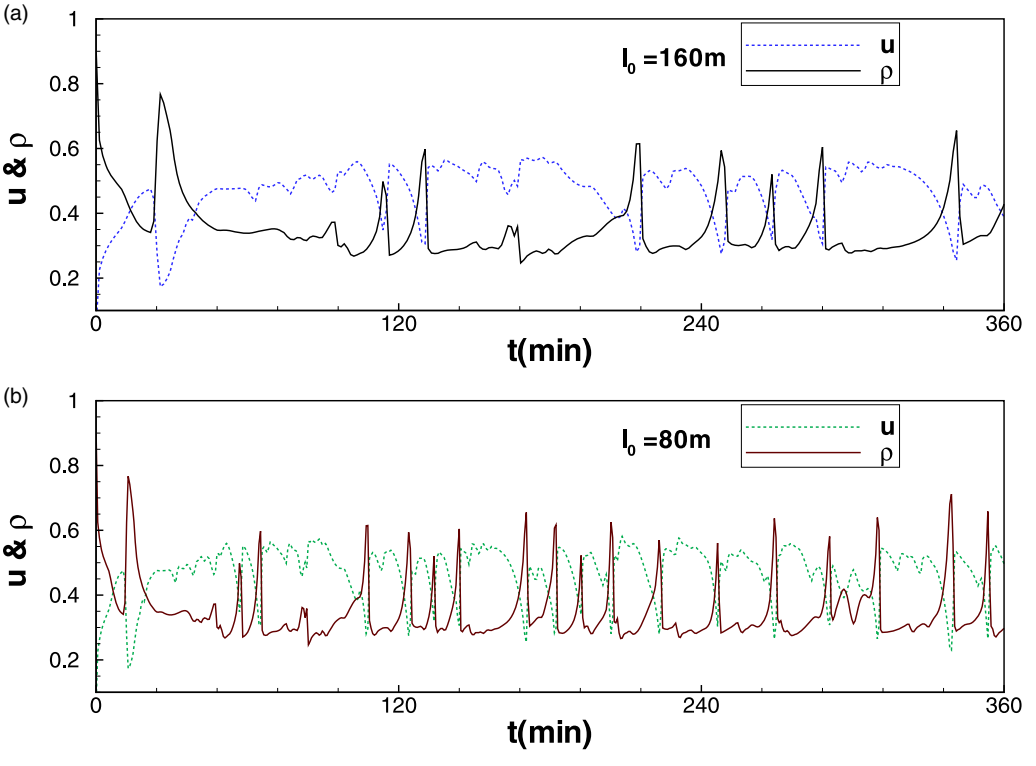

Figure 10. Evolutions of traffic speed and density at $x = 375$ for $l_0 = 160$ m (a) and 80 m (b), respectively.

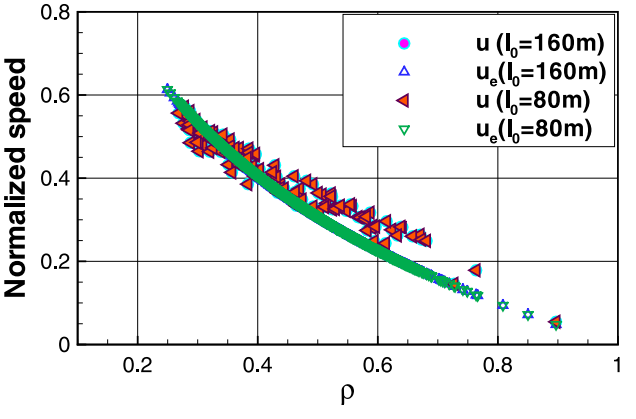

Figure 11. Comparison of traffic speed–density relation at $x = 375$ for $l_0 = 160$ m and 80 m, respectively.

To demonstrate the sensitivity of characteristic length more clearly, similar to Section 5.4, the temporal evolutions of speed and density at $x = 375$ are again illustrated, as seen in Figure 10(a) and 10(b). The structures of speed and density waves differ from each other, differences can be viewed by comparing their wave magnitude and wavelength.

Although relaxation time decreases with the characteristic length, the first critical density remains the same, the temporal evolutions of speed and density are determinatively impacted by the relaxation time, comparison of the relation of instantaneous and equilibrium speeds to density reveals rather smaller discrepancy, as shown in Figure 11, indicating that the impact of fundamental diagram curve is dramatically large, similar to traffic viscoelasticity.

6. Conclusions

A fluid dynamic type viscoelastic traffic flow model is briefly reported and employed to explore traffic flow sensitivity to the model parameters by virtue of numerical simulation of ring traffic flows. Numerical results revealed the following findings:

(1) Traffic flow pattern formation is dramatically sensitive to viscoelasticity, and so is the fundamental diagram curve which is explicitly impacted by average vehicle length and braking distance, implying that drivers' self-organisation ability is significant in determining the intensity of traffic wave interaction.
(2) Even though the transitional density is insensitive to traffic characteristic length, the decrease in the characteristic length can lead to a relevant change of traffic relaxation time. This length is also a sensitive feature of changing traffic wave structures.
(3) It is necessary to optimise traffic flow regulations for the purpose of keeping a segmental or ring road working in an expected operational environment.

Disclosure statement

No potential conflict of interest was reported by the authors.

Funding information

This work is supported by Russian Foundation for Basic Research [RFBR 13-01-12056] and NSFC [10972212].

References

Aw, A., and M. Rascle. 2000. "Resurrection of 'Second Order' Models of Traffic Flow." *SIAM Journal on Applied Mathematics* 60: 916–938.

Bogdanova, A., M. N. Smirnova, Z. J. Zhu, and N. N. Smirnov. 2015. "Exploring Peculiarities of Traffic Flows with a Viscoelastic Model." *Transportmetrica A: Transport Science*. doi:10.1080/23249935.2015.1030472.

Castillo, J. M. D. 2001. "Propagation of Perturbations in Dense Traffic Flow: A Model and Its Implications." *Transportation Research Part B: Methodological* 35: 367–389.

Castillo, J. M. D., and F. G. Benitez. 1995a. "On the Functional Form of the Speed–Density Relationship I: General Theory." *Transportation Research Part B: Methodological* 29 (5): 373–389.

Castillo, J. M. D., and F. G. Benitez. 1995b. "On the Functional Form of the Speed–Density Relationship II: Empirical Investigation." *Transportation Research Part B: Methodological* 29 (5): 391–406.

Chandrasekhar, S. 1961. "Basic Concepts." In *Hydrodynamic and Hydromagnetic Stability*, edited by S. Chandrasekhar, 1–7. London: Oxford University Press.

Chang, G.-L., and Z. J. Zhu. 2006. "A Macroscopic Traffic Model for Highway Work Zones: Formulations and Numerical Results." *Journal of Advanced Transportation* 40 (3): 265–287.

Costeseque, G., and J. P. Lebacque. 2014. "A Variational Formulation for Higher Order Macroscopic Traffic Flow Models: Numerical Investigation." *Transportation Research Part B: Methodological* 70: 112–133.

Daganzo, C. F. 1995. "Requiem for Second-order Fluid Approximations of Traffic Flow." *Transportation Research Part B: Methodological* 29: 277–286.

Daganzo, C. F. 1997. "Traffic Flow Theory." In *Fundamentals of Transportation and Traffic Operations*, edited by C. F. Daganzo, 67–160. New York: Pergamon.

Delis, A. I., I. K. Nikolos, and M. Papageorgiou. 2014. "High-resolution Numerical Relaxation Approximations to Second-order Macroscopic Traffic Flow Models." *Transportation Research Part C: Emerging Technologies* 44: 318–349.
Haight, F. A. 1963. "Fundamental Characteristics of Road Traffic." In *Mathematical Theories of Traffic Flow*, edited by F. A. Haight, 67–89. London: Academic Press.
Han, S. F. 2000. "Constitutive Theory of Viscoelastic Fluids." In *Constitutive Equation and Computational Analytical Theory of Non-Newtonian Fluid*, edited by S. F. Han, 59–86. Peking: Science Press.
Helbing, D. 2001. "Traffic and Related Self-driven Many-particle Systems." *Reviews of Modern Physics* 73: 1067–1141.
Helbing, D., A. Hennecke, and M. Treiber. 1999. "Phase Diagram of Traffic States in the Presence of Inhomogeneities." *Physical Review Letters* 82 (21): 4360–4363.
Helbing, D., and M. Treiber. 1998. "Gas-kinetic-based Traffic Model Explaining Observed Hysteretic Phase Transition." *Physical Review Letters* 81: 3042–3045.
Hilliges, M., and W. Weidlich. 1995. "A Phenomenological Model for Dynamic Traffic Flow in Networks." *Transportation Research Part B: Methodological*. 29 (6): 407–431.
Hoogendoorn, S. P., and P. H. L. Bovy. 2000. "Continuum Modeling of Multiclass Traffic Flow." *Transportation Research Part B: Methodological* 34 (2): 123–146.
Hoogendoorn, S. P., F. van Wageningen-Kessels, W. Daamen, D. C. Duives, and M. Sarvi. 2016. "Continuum Theory for Pedestrian Traffic Flow: Local Route Choice Modelling and Its Implications." *Transportation Research Part C: Emerging Technologies* 59: 183–197.
Jiang, G.-S., and C.-W. Shu. 1996. "Efficient Implementation of Weighted Eno Schemes." *Journal of Computational Physics* 126: 202–228.
Kerner, B., and P. Konhäuser. 1993. "Cluster Effect in Initially Homogemeous Traffic Flow." *Physical Review E* 48: 2335–2338.
Kiselev, A. B., A. V. Kokoreva, V. F. Nikitin, and N. N. Smirnov. 2004. "Mathematical Modelling of Traffic Flows on Controled Roads." *Journal of Applied Mathematics and Mechanics* 68: 933–939.
Kiselev, A. B., V. F. Nikitin, N. N. Smirnov, and M. V. Yumashev. 2000. "Irregular Traffic Flow on a Ring Road." *Journal of Applied Mathematics and Mechanics* 64 (4): 627–634.
Klar, A., and R. Wegener. 2000. "Kinetic Derivation of Macroscopic Anticipation Models for Vehicular Traffic." *SIAM Journal of Applied Mathematics* 60 (5): 1749–1766.
Kuhne, R. D., and P. Michalopoulos. 2001. "Continuum Flow Models." Printed at http://www-cta.ornl.gov/cta/research/trb/tft.html.
Lebacque, J.-P., and M. M. Khoshyaran. 2013. "A Variational Formulation for Higher Order Macroscopic Traffic Flow Models of the GSOM Family." *Transportation Research Part B: Methodological* 57: 245–265.
Lebacque, J.-P., S. Mammar, and H. Haj-Salem. 2007a. "The Aw-Rascle and Zhang's Model: Vacuum Problems, Existence and Regularity of the Solutions of Riemann Problem." *Transportation Research Part B: Methodological* 41 (7): 710–721.
Lebacque, J.-P., S. Mammar, and H. Haj-Salem. 2007b. "Generic Second Order Traffic Flow Modelling." In *Transportation and Traffic Theory*, edited by R. Allsop and G. Benjiamin, 755–776. Oxford: Elsevier.
Li, T. 2008. "Stability of Traveling Waves in Quasi-linear Hyperbolic Systems with Relaxation and Diffusion." *SIAM Journal of Mathematical Analysis* 40 (3): 1058–1075.
Lighthill, M. J., and G. B. Whitham. 1955. "On Kinematic Waves. II. A Theory of Traffic Flow on Long Crowded Roads." *Proceedings of the Royal Society of London A* 229: 317–345.
Liu, G. Q., and A. S. Lyrintzis. 1996. "Modelling of Freeway Merging and Diverging Flow Dynamics." *Applied Mathematical Modelling* 229: 317–345.
Lu, Y. D., S. C. Wong, M. P. Zhang, and C.-W. Shu. 2009. "The Entropy Solutions for the Lighthill–Whitham–Richards Traffic Flow Model with a Discontinuous Flow–Density Relationship." *Transportation Science* 43 (4): 511–530.
Mammar, S., J.-P. Lebacque, and H. H. Salem. 2009. "Riemann Problem Resolution and Godunov Scheme for the Aw-Rascle-Zhang Model." *Transportation Science* 43 (4): 531–545.
McShane, W. R., R. P. Roess, and E. S. Prassas. 1998. "Calibration Relationships for Freeway Analysis." In *Traffic Engineering*, edited by W. R. McShane, R. P. Roess, and E. S. Prassas, 282–306. New Jersey, NJ: Prentice-Hall.
Michalopoulos, P. G., D. E. Beskos, and J.-K. Lin. 1984. "Analysis of Interrupted Traffic Flow by Finite Difference Methods." *Transportation Research Part B: Methodological* 18 (4–5): 409–421.
Ngoduy, D. 2012. "Application of Gas-kinetic Theory to Modelling Mixed Traffic of Manual and Adaptive Cruise Control Vehicles." *Transportmetrica Part A: Transport Science* 8 (1): 43–60.
Ngoduy, D. 2013. "Platoon-based Macroscopic Model for Intelligent Traffic Flow." *Transportmetrica B: Transport Dynamics* 1 (2): 153–169.
Ou, Z. H., and S. Q. Dai. 2006. "Nonlinear Analysis in the Aw-Rascle Anticipation Model of Traffic Flow." *SIAM Journal of Applied Mathematics* 67 (3): 605–618.
Papageorgiou, M., and J. M. Blosseville. 1989. "Macroscopic Modeling of Traffic Flow on the Boulevard Périphérique in Paris." *Transportation Research Part B: Methodological* 23 (1): 29–47.
Payne, H. J. 1971. "Models of Freeway Traffic and Control." Mathematical model of public systems, simulation council proceedings, La Jola, CA, Vol. 1, 51–61.
Payne, H. J. 1979. "Freflo: A Macroscopic Simulation Model of Freewaytraffic." *Transportation Research Record* 722: 68–77.
Richards, P. I. 1956. "Shock Waves on the Highway." *Operations Research* 4: 42–51.

Roe, P. C. 1981. "Approximate Riemann Solvers, Parameter Vectors, and Difference Schemes." *Journal of Computational Physics* 43: 357–372.
Schönhof, M., and D. Helbing. 2009. "Criticism of Three-phase Traffic Theory." *Transportation Research Part B: Methodological* 43: 784–797.
Shui, H. S. 1998. "TVD Scheme." In *Finite Difference in One-dimensional Fluid Mechanics*, edited by H. S. Shui, 333–355. Beijing: National Defense [in Chinese].
Smirnov, N. N., A. B. Kiselev, V. F. Nikitin, M. V. Silnikov, and A. S. Manenkova. 2014. "Hydrodynamic Traffic Flow Models and Its Application to Studying Traffic Control Effectiveness." *WSEAS Transactions on Fluid Mechanics* 9: 178–186.
Smirnova, M. N., A. I. Bogdanova, N. N. Smirnov, A. B. Kiselev, V. F. Nikitin, and A. S. Manenkova. 2014a. "Multi-lane Unsteady-state Traffic Flow Models." *Journal of Mechatronics* 2 (4): 1–5.
Smirnova, M. N., A. I. Bogdanova, N. N. Smirnov, A. B. Kiselev, V. F. Nikitin, and A. S. Manenkova. In press. "Unsteady-state Traffic Flow Models for Urban Regulation Strategy Planning." *Architecture and Urban Design*.
Smirnova, M. N., A. I. Bogdanova, Z. J. Zhu, A. S. Manenkova, and N. N. Smirnov. 2014b. "Mathematical Modeling of Traffic Flows Using Continuum Approach. Visco-elastic Effect in Traffic Flows." *Mathematical Modeling* 26 (7): 54–64 (in Russian).
Spiliopoulou, A., M. Kontorinaki, M. Papageorgiou, and P. Kopelias. 2014. "Macroscopic Traffic Flow Model Validation at Congested Freeway Off-Ramp Areas." *Transportation Research Part C: Emerging Technological* 41: 18–29.
Tordeux, A., M. Roussignol, J. P. Lebacque, and S. Lassarre. 2014. "A Stochastic Jump Process Applied to Traffic Flow Modelling." *Transportmetrica A: Transport Science* 10 (4): 350–375.
Wagner, M. H. 1978. "A Constitutive Analysis of Uniaxial Elongational Flow Data of Low-density Polyethylene Melt." *Journal of Non-Newtonian Fluid* 4 (1–2): 39–55.
Whitham, G. B. 1974. *Linear and Nonlinear Waves*. New York: Wiley.
Wong, G. C. K., and S. C. Wong. 2002. "A Multi-class Traffic Flow Model – An Extension of LWR Model with Heterogeneous Drivers." *Transportation Research Part A: Policy and Practice* 36: 827–841.
Zhang, H. M. 2003. "Driver Memory, Traffic Viscosity and a Viscous Vehicular Traffic Flow Model." *Transportation Research Part B: Methodological* 37: 27–41.
Zhang, P., and S. C. Wong. 2006. "Essence of Conservation Forms in the Travelling Wave Solutions of Higher-order Traffic Flow Models." *Physical Review E* 74 (2): 026109.
Zhang, P., S. C. Wong, and S. Q. Dai. 2009. "A Conserved Higher Order Anisotropic Traffic Flow Model: Description of Equilibrium and Non-equilibrium Flows." *Transportation Research Part B: Methodological* 43 (5): 562–574.
Zhu, Z. J., and T. Q. Wu. 2003. "Two-phase Fluids Model for Freeway Traffic Flow and Its Application to Simulate the Evolution of Solitons in Traffic." *ASCE, Journal of Transportation Engineering* 129: 51–56.
Zhu, Z. J., Q. S. Wu, R. Jiang, and T. Wu. 2002. "Numerical Study on Traffic Flow with Single Parameter State Equation." *ASCE, Journal of Transportation Engineering* 128: 167–172.
Zhu, Z., and C. Yang. 2013. "Visco-elastic Traffic Flow Model." *Journal of Advanced Transportation* 47: 635–649.

Appendix 1. Relation between $\mathbf{B}_n$ and $\mathbf{B}_{n+1}$

In Chapter II of Han (2000), it was reported that for $n \geq 1$:

$$\mathbf{B}_{n+1}(s) = \mathrm{d}\mathbf{B}_n/\mathrm{d}s - \mathbf{L}_1\mathbf{B}_n - \mathbf{B}_n\mathbf{L}_1^{\mathrm{T}} \tag{A1}$$

where $\mathbf{L}_1 = \nabla\mathbf{u}$, $\mathbf{L}_1^{\mathrm{T}}$ is the transposition of $\mathbf{L}_1$. $\mathbf{B}_0 = 1$, and $\mathbf{B}_1 = \mathbf{L}_1 + \mathbf{L}_1^{\mathrm{T}}$.

Appendix 2. Pressure derivation

Remembering the assumption for traffic pressure, and denoting average vehicle length by l, we have:

$$p \propto \frac{1}{s - l} \tag{A2}$$

where $s = 1/\rho$. Assume $\alpha = l\rho_m$, traffic pressure can be expressed as:

$$p \propto \frac{\rho}{1 - \alpha\rho/\rho_m} \tag{A3}$$

Let the jam pressure be p_m, it has the form:

$$p = p_m(1 - \alpha)(\rho/\rho_m)/[1 - \alpha(\rho/\rho_m)] \tag{A4}$$

Therefore, the sound speed can be expressed as:

$$c^2 = \frac{\partial p}{\partial \rho} = c_0^2(1-\alpha)/(1-\alpha\rho/\rho_m)^2 \tag{A5}$$

where, as given by Equation (11):

$$c_0^2 = \frac{(1-\alpha\rho_*/\rho_m)\rho_*/\rho_m}{2(1-\rho_*/\rho_m)} v_f^2$$